Superoleophobic behavior of fluorinated conductive polymer films combining electropolymerization and lithography

Thierry Darmanin,[a] Frederic Guittard,*[a] Sonia Amigoni,[a] Elisabeth Tafin de Givenchy,[a] Xavier Noblin,[b] Richard Kofman[b] and Franck Celestini[b]

Received 18th August 2010, Accepted 28th October 2010
DOI: 10.1039/c0sm00837k

The surface construction to reach super oil non-wetting properties is very complex because of the necessary force for impeding the natural spreading of low surface tension oils. Here, a polymer, which is able to reach the superoleophobicity when it is electrodeposited on smooth surfaces, has been deposited on micro-patterned substrates made of cylindrical arrays (∅: 13 μm, H: 25 μm, distance between cylinders: 40 μm) in order to determine the effect of the pattern on the super oil-repellency properties. The surface analysis using various oils has shown that the pattern used highly decreases the time of deposition and, as a consequence, the required amount of polymer to obtain anti-oil surfaces. This work is the first step in the short term prospects for the elaboration of superoleophobic surfaces combining electropolymerization with lithography.

1. Introduction

Superoleophobic surfaces, which repel oils, are very difficult to design due to the low surface tension of these liquids. There are only a few publications[1–22] on this subject in opposition to the literature of superhydrophobic surfaces which have concerned up to now more than one thousand publications. While superhydrophobic surfaces are made by combining two elements, the surface roughness and a hydrophobic part,[23–27] in most cases, this is not sufficient to reach superoleophobicity. In the literature, the superoleophobic properties are very dependent on the oils used for the measurements and more precisely on their surface tensions: it is now established that the surface non-wetting properties decrease with the surface tension of the liquid. If it is admitted that a surface is superhydrophobic when the contact angle with pure water is higher than 150°, which oil should be used to describe superoleophobicity? Thus, among the literature, it is very difficult to know which surfaces are truly superoleophobic because many oils were used such as octane (21.6 mN m^{-1}),[4] hexadecane (27.6 mN m^{-1}),[1–3,11,12,14,17] rapeseed oil (35.0 mN m^{-1}),[15,16] salad oil (33.0 mN m^{-1})[3c,9] or xylene (29.0 mN m^{-1}) and sometimes the oil nature is not mentioned.[8,10,18] Sometimes the authors claimed superoleophobic properties using liquids which are not oils like diiodomethane (50.8 mN m^{-1})[13,21,22] or glycerol (64.0 mN m^{-1}).[21] The term superlyophobic[7] has also been employed for the repellency from 21.8 mN m^{-1} surface tension of liquids (ethanol) to 72.0 mN m^{-1} (water) and sometimes also the term superamphiphobic.[8–10,13,15,16,18,22] Finally, dynamic contact angles (advancing and receding contact angles) and sliding angles, which are very important to determine the non-wetting properties, are often missing. An important work has been reported by Tuteja *et al.* They elaborated surfaces, from photolithography process, which exhibited highly superoleophobic properties and repelled even octane.[4] These exceptional properties were due to "re-entrant" geometries,[4–7,28,29] and the behavior of oils on these surfaces was very dependent on the surface topography.

Electropolymerization is a fast method for the deposition of conductive polymers on conductive electrodes (gold, platinum, stainless steel,…). Following the electrochemical conditions and the chemical structure of the monomer, structured superhydrophobic films could be directly obtained.[30–35] Using this method, superhydrophobic polypyrrole,[30–33] polythiophene,[34] poly(3,4-ethylenedioxythiophene)[35] films showing exceptional non-wetting properties were reported. Recently, we found a way for superoleophobicity by molecular design of conductive polymers. In particular, fluorinated 3,4-ethylenedioxypyrrole (EDOP) derivatives are excellent candidates.[1,2] Their electropolymerization using appropriate conditions and on smooth gold surfaces allowed to reach self-cleaning properties with hexadecane. As the adhesion of hexadecane droplets was very low due to the presence of surface nanoporosity, they could roll off the surfaces very easily (sliding angle < 12°).

Mimicking nature, the improvement of the surface hydrophobicity is often realized by combining micro- and nanostructures on the surface. For example, the self-cleaning properties of lotus leaves,[36,37] the antifogging properties of the eyes of the mosquito *Culex pipiens*[38] and the "petal effect" of red roses[39] are the consequences of surface topography consisting in both micro- and nanostructures. These observations and the understanding of the complex problems of liquid-repellency have allowed to obtain surfaces with exceptional water-repellent properties and extremely low hysteresis.[40–45] However, few works reported on the elaboration of superoleophobic surfaces with both micro- and nanostructures. Bioinspired by the surface structures of fish scales, Jiang *et al.* have elaborated

---

[a] *Université de Nice Sophia-Antipolis, Laboratoire de Chimie des Matériaux Organiques et Métalliques, EA 3155, Equipe Chimie Organique aux Interfaces, Parc Valrose, 06108 Nice Cedex 2, France. E-mail: Frederic.GUITTARD@unice.fr; Fax: +33 4-92-07-61-56; Tel: +33 4-92-07-61-59*
[b] *Université de Nice Sophia-Antipolis, Laboratoire de Physique de la Matière Condensée, UMR 6622, CNRS, Parc Valrose, 06108 Nice Cedex 2, France*

micro/nanostructure silicon surfaces exhibiting superoleophobic properties but only if the surface was immerged in water.[20] Superoleophobic cotton textiles based on multilength-scale roughness were obtained by grafting silica microparticles and nanoparticles on the fibers.[17]

Here, we investigate the effect of a microstructured topography, consisting in arrays of cylindrical micro-pillars (Fig. 1a), on nanoporous fluorinated poly(3,4-ethylenedioxypyrrole) films, which exhibit already the superoleophobic properties when electrodeposited on smooth surfaces. The monomer used for the electropolymerization is represented in Fig. 1b. The surface properties were investigated by contact angle measurements (static, advancing and receding contact angle, sliding angle) using different oils (pentane, hexane, heptane, octane, decane, dodecane, hexadecane and sunflower oil) and by scanning electron microscopy.

2. Experimental

2.1. Elaboration of micro-plotted surfaces

The micro-plot arrays (Fig. 1a) were fabricated using regular photolithography[46] using an SU-8 photoresist (SU-8 2025, Microchem, Newton, MA, USA). By UV exposure through a mask, square arrays of cylinders (13 μm diameter, distance between cylinders: 40 μm) were fabricated over 2 × 2 cm areas on silicon wafers. The cylinders height was 25 μm, given by the SU-8 layer deposited by spin-coating. After formation of the micropillars, the surfaces were modified to become conductive for the electrochemical deposition of the polymer film. For this, 50 nm gold film was deposited on the microstructured surface by evaporation–condensation under UHV. Finally a copper wire was cold-soldered on the gold surfaces at the edge of silicon wafer to connect them electrically to the electrodeposition apparatus

2.2. Electropolymerization

The synthesis of the monomer, shown in Fig. 1b, was already reported in the literature.[47] For the electrochemical polymerization, the monomer (0.005 M) was dissolved in a previously degassed acetonitrile solution containing 0.1 M of tetrabutylammonium hexafluorophosphate. The polymer films were electrodeposited on the micro-patterned gold working electrode by applying a constant potential of 0.82 V *vs.* saturated calomel electrode (SCE) with various deposition charge, Qs (mC cm^{-2}), corresponding to different amounts of polymer. The electrochemical system was composed of a gold plate (with or without pattern) as a working electrode, a glassy carbon rod as a counter-electrode and a SCE reference electrode. These three electrodes were connected to an Autolab PGSTAT 30 potentiostat from Eco Chemie B.V. The software General Purpose Electrochemical System GPES was used for the measurements.

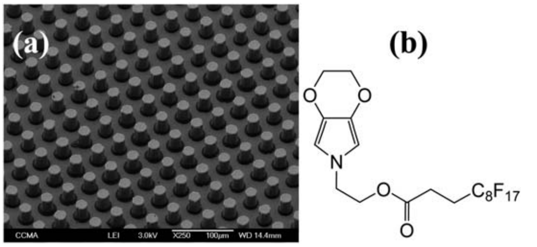

Fig. 1 (a) SEM image of the micro-pillars surface and (b) monomer used for the electropolymerization.

2.3. Surface characterization

The wettability study was performed using seven hydrocarbons of different surface tensions and also sunflower oil, which contains various hydrocarbons. The static contact angles were determined by depositing 2 μL droplets on the surfaces and analyzing with a Krüss DSA-10 contact angle goniometer. For the dynamic contact angles, 6 μL droplets were deposited on the surfaces, after that the surfaces were inclined until the droplet rolled off the surface. The angle of inclination is named sliding angle. By filming the experiments, the advancing and receding contact angles were evaluated just before the droplet rolled off the surface (the inclination deforms the droplet). All data correspond to an average of five measurements at 21 ± 1 °C. The SEM images were obtained with a JEOL 6700F microscope.

3. Results and discussion

The static (equilibrium) hexadecane contact angles as a function of the deposition charge are represented in Fig. 2 and Table 1. It shows that it is possible to reach static contact angles with hexadecane up to 145° with or without the micropillars. Besides, the presence of the pillars led to a drastic decrease of the necessary charge, that is to say the polymer amount, to obtain the optimal oil contact angles. Indeed, whereas on smooth surfaces a deposition charge of 225 mC cm^{-2} was necessary to obtain the optimal oleophobicity, with the presence of the pillars a deposition charge of 25 mC cm^{-2} was sufficient to reach the 145° plateau. Thus, the pillars allowed the reduction of necessary amount of polymer by 10 and therefore highly reduced the cost and time of deposition. Fig. 2 also shows that for Qs = 10 mC cm^{-2}, the presence of pillars can switch the surface wettability from oleophilic (71° on smooth surfaces) to oleophobic (130° on microstructured surfaces). Indeed, Zhou *et al.*[48] already showed that

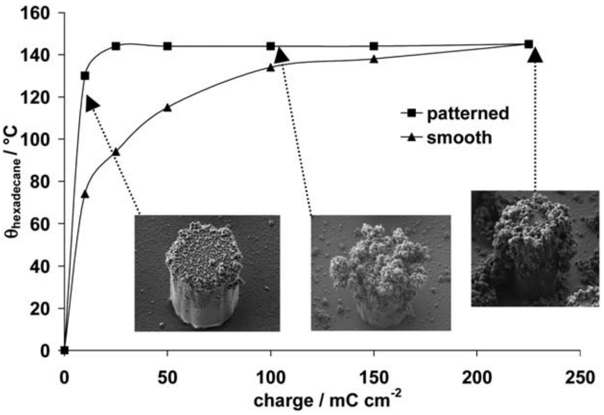

Fig. 2 Static hexadecane contact angles of the polymer electrodeposited films on micro-patterned (■) and smooth (▲) gold surfaces as a function of the deposition charge. Insets: SEM images of the pillars as a function of the deposition charge (12.5, 100 and 225 mC cm^{-2}).

Table 1 Static and dynamic contact angles with hexadecane, measured on polymer films electrodeposited on the micro-patterned surface, as a function of the deposition charge

Deposition charge Qs/mC cm^{-2}	Static hexadecane contact angle/°	Dynamic contact angle with hexadecane/°			
		Advancing contact angle	Receding contact angle	Hysteresis	Sliding angle
0	0	—	—	—	No sliding angle
10	130	—	—	—	No sliding angle
25	144	158	115	43	34
50	145	155	117	38	25
100	144	155	115	40	26
150	144	153	115	38	26
225	144	153	118	35	27

some rough solid surface like pillar structure could lead to super water-repellency (contact angle larger than 150 degree), although the smooth or flat surface of the same material showed a contact angle less than 90 degree. The phenomenon cannot be explained directly by Wenzel or Cassie-Baxter models[49] and a "pinning effect" as well as the concept of metastable states of the wetting were introduced.[50] Some metastable states also are induced by "re-entrant" surface geometries.[4b]

Dynamic contact angle measurements with hexadecane revealed the average hysteresis ($H \approx 40^\circ$) and sliding angle ($\alpha \approx 26^\circ$) measured on the patterned surfaces were both higher than deposited on smooth surfaces ($H \approx 22^\circ$, $\alpha \approx 12^\circ$) showing a higher adhesion of hexadecane droplets (6 μL) with the pattern. Fig. 3 shows the surface morphology observed for a deposition charge of Qs = 225 mC cm^{-2}. The whole surfaces were covered by the polymer. The polymer continuously grew on the cylinders and in between but when the polymer amount became significant, polymer bridges were formed between them, which changed the surface topography (Fig. 3c).

Fig. 3d confirms the presence of nanoporosity within the electrodeposited film as already observed previously on smooth gold surfaces.[1,2] The formation of the surface nanoporosity was attributed to the doping process of the polymer during the electropolymerization.[1] However, the polymer coverage was not uniform: the deposit was thin at the bottom of the pillars while it was thick on top of them, in particular on the edges. Continuity between these two conductive regions (bottom and top of the pillars) existed due to a small quantity of gold deposited on the pillar walls and was demonstrated by the presence of electrodeposited polymer on the two regions as shown in insets of Fig. 2. The deposit was thicker where the current density in the electrolyte was higher *i.e.* where the electric field was higher (Ohm's law). However, it is known that the electric field is higher on high curvature surfaces (point effect) like on the edges on top of them. The conductive plane which supports the pillars was screened by the top of the pillars (equipotential surfaces were curved and distant between the pillars); the electric field on the base plane was of lower magnitude than on top of the cylinders and the deposit was then reduced.

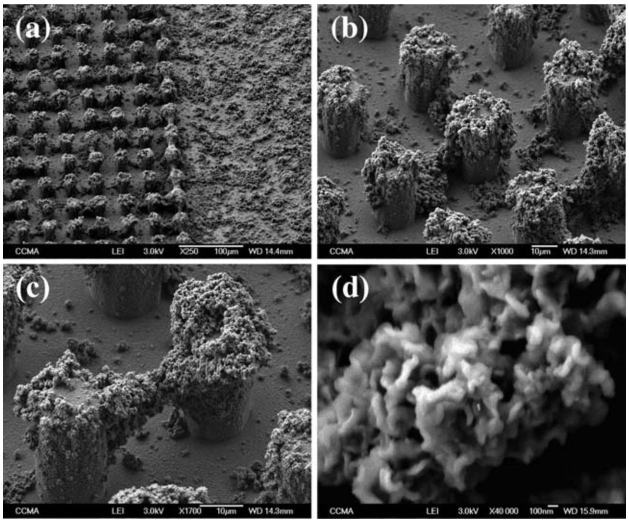

Fig. 3 SEM images of patterned gold surfaces electrochemically coated by the fluorinated polymer; the scale bar represents (a) 100 μm, (b and c) 10 μm, (d) 100 nm (Qs = 225 mC cm^{-2}).

The evolution of the static contact angles as a function of the surface tension of the liquid probe is shown in Fig. 4 and Table 2.

First of all, we can point out that the tendencies for the two curves are identical; this means that a charge of 100 mC cm^{-2} on the patterned surface was sufficient to equal the properties attained by a charge twice high (225 mC cm^{-2}) on the flat surface. Indeed, in both cases, the contact angles increased promptly with the oil surface tensions to reach a plateau. On the plateau, *i.e.* for liquids with surface tension higher than 30 mN m^{-1}, such as sunflower oil (31 mN m^{-1}), diiodomethane (50.8 mN m^{-1}) or water (72.0 mN m^{-1}), the liquid droplets did not penetrate the spaces between the micro-pillars and the presence of the

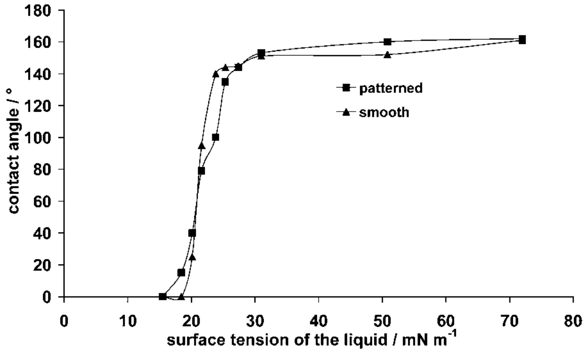

Fig. 4 Static contact angles of the polymer films electrodeposited on micro-patterned (Qs = 100 mC cm^{-2}) and smooth gold surfaces (Qs = 225 mC cm^{-2}) and as a function of the surface tension of the liquid probe.

Table 2 Dynamic contact angles, measured on polymer films electrodeposited on the micro-patterned surface, as a function of the surface tension of the liquid probe (Qs = 100 mC cm^{-2})

			Dynamic contact angle/°			
Liquid probe	Surface tension/mN m^{-1}	Static contact angle/°	Advancing contact angle	Receding contact angle	Hysteresis	Sliding angle
Sunflower oil	~31	153	155	148	4	3
Hexadecane	27.6	144	155	115	40	26
Dodecane	25.3	135	—	—	—	No sliding angle
Decane	23.8	100	—	—	—	No sliding angle
octane	21.6	84	—	—	—	No sliding angle
Heptane	20.1	40	—	—	—	No sliding angle
Hexane	18.4	15	—	—	—	No sliding angle
Pentane	15.5	0	—	—	—	No sliding angle

microstructuring improved the non-wetting properties. It is confirmed by both the low hysteresis (≤4°) and sliding angle (≤3°) measured from these liquids with surface tension up to 30 mN m^{-1}. In contrast, hexadecane (27.6 mN m^{-1}) seemed to penetrate between the micro-pillars leading to a noticeable increase of both hysteresis ($H = 40°$) and sliding angle ($\alpha = 26°$). Finally, when the surface tension of the liquid became lower (≤25 mN m^{-1}), the oleophilicity increased ($\gamma_{\text{oil}} \leq 21$ mN m^{-1}) or decreased ($\gamma_{\text{oil}} \geq 21$ mN m^{-1}) with the surface structuring and the liquid droplets stuck to the surface (hysteresis and sliding angle were thus not measurable with the tilted-drop method) due to higher penetration of the liquids between the pillars.

In our case, the measurements showed that the superoleophobic properties are mostly given by the nanoporosity of the fluorinated electrodeposited film; the micro-structuration of the gold surface has just an influence on the needed amount of oleophobic polymer. If previous works showed that nanostructuring surface is one parameter that can govern the superlyophobic properties, here we point out that the level of microstructuring is very important to enhance the ability of the nanoscale to support oil liquid. In order to significantly increase the maximum contact angle with low surface tension liquids we plan, in a near future, to work on the size of the pillars as well as the distance between them. This will aim at improving the surface oleophobicity without using too complex surface topographies, such as re-entrant curvatures.[4–7,28,29]

Conclusions

We have electrodeposited nanoporous superoleophobic films made of fluorinated poly(3,4-ethylenedioxypyrroles) on micropatterned gold surface consisting in arrays of cylindrical micropillars (∅: 13 μm, H: 25 μm, distance between cylinders: 40 μm) and the resulting surfaces have been characterized with different oils in order to determine the effect of the pattern on the super oil-repellent properties. We have shown that, in our case, the micro-pattern allows to obtain the superoleophobic properties much faster, which reduces the time of deposition and the amount of polymer. Therefore, the micro-pattern allows to reach superoleophobic properties at low deposition charge. However, the micro-pattern does not induce an increase of the maximum contact angles of oils and even a slight diminution has been measured using oils of extremely low surface tension. Thus, if it is known that a surface microstructuration can easily increase the surface hydrophobicity, this is not the case for the surface oleophobicity. Others patterns, probably more complex and with different size and spacing, will be used in the future in order to confirm these results and improve the surface oleophobicity.

Notes and references

1 (*a*) T. Darmanin and F. Guittard, *J. Am. Chem. Soc.*, 2009, **131**, 7928; (*b*) T. Darmanin and F. Guittard, *J. Mater. Chem.*, 2009, **19**, 7130.
2 A. Zenerino, T. Darmanin, E. Taffin de Givenchy, S. Amigoni and F. Guittard, *Langmuir*, 2010, **26**, 13545.
3 (*a*) K. Tsujii, T. Yamamoto, T. Onda and S. Shibuichi, *Angew. Chem., Int. Ed. Engl.*, 1997, **36**, 1011; (*b*) S. Shibuichi, T. Yamamoto, T. Onda and K. Tsujii, *J. Colloid Interface Sci.*, 1998, **208**, 287; (*c*) H. Yan, K. Kurogi and K. Tsujii, *Colloids Surf., A*, 2007, **292**, 27.
4 (*a*) A. Tuteja, W. Choi, M. Ma, J. M. Mabry, S. A. Mazzella, G. C. Rutledge, G. H. McKinley and R. E. Cohen, *Science*, 2007, **318**, 1618; (*b*) W. Choi, A. Tuteja, S. Chhatre, J. M. Mabry, R. E. Cohen and G. H. McKinley, *Adv. Mater.*, 2009, **21**, 2190.
5 L. Joly and T. Biben, *Soft Matter*, 2009, **5**, 2549.
6 A. Marmur, *Langmuir*, 2008, **24**, 7573.
7 A. Ahuja, J. A. Taylor, V. Lifton, A. A. Sidorenko, T. R. Salamon, E. J. Lobaton, P. Kolodner and T. N. Krupenkin, *Langmuir*, 2008, **24**, 9.
8 Y. Tian, H. Liu and Z. Deng, *Chem. Mater.*, 2006, **18**, 5820.
9 J. Xi, L. Feng and L. Jiang, *Appl. Phys. Lett.*, 2008, 92053102.
10 Q. Xie, J. Xu, L. Feng, L. Jiang, W. Tang, X. Luo and C. C. Han, *Adv. Mater.*, 2004, **16**, 302.
11 J. Zimmermann, M. Rabe, G. R. J. Artus and S. Seeger, *Soft Matter*, 2008, **4**, 450.
12 L. Cao, T. P. Price, M. Weiss and D. Gao, *Langmuir*, 2008, **24**, 1640.
13 C.-F. Wang, F.-H. Chiou, F.-H. Ko, C.-T. Chou, H.-C. Lin, C.-F. Huang and F.-C. Chang, *Macromol. Rapid Commun.*, 2006, **27**, 333.
14 W. Chen, A. Y. Fadeev, M. C. Hsieh, D. Oner, J. Youngblood and T. J. McCarthy, *Langmuir*, 1999, **15**, 3395.
15 H. Li, X. Wang, Y. Song, Y. Liu, Q. Li, L. Jiang and D. Zhu, *Angew. Chem., Int. Ed.*, 2001, **40**, 1743.
16 H. Meng, S. Wang, J. Xi, Z. Tang and L. Jiang, *J. Phys. Chem. C*, 2008, **112**, 11454.
17 B. Leng, Z. Shao, G. With and W. Ming, *Langmuir*, 2009, **25**, 2456.
18 K. Zhao, K. S. Liu, J. F. Li, W. H. Wang and L. Jiang, *Scr. Mater.*, 2009, **60**, 225.
19 A. Steele, I. Bayer and E. Loth, *Nano Lett.*, 2009, **9**, 501.
20 M. Liu, S. Wang, Z. Wei, Y. Song and L. Jiang, *Adv. Mater.*, 2009, **21**, 665.
21 X. Liu, W. Wu, X. Wang, Z. Z. Luo, Y. Liang and F. Zhou, *Soft Matter*, 2009, **5**, 3097.
22 (*a*) Y.-C. Sheen, Y.-C. Huang, C.-S. Liao, H.-Y. Chou and F.-C. Chang, *J. Polym. Sci., Part B: Polym. Phys.*, 2008, **46**, 1984; (*b*) Y.-C. Sheen, W.-H. Chang, W.-C. Chen, Y.-H. Chang, Y.-C. Huang and F.-C. Chang, *Mater. Chem. Phys.*, 2009, **114**, 63.
23 X. Zhang, F. Shi, J. Niu, Y. Jiang and Z. J. Wang, *J. Mater. Chem.*, 2008, **18**, 621.

24 X.-M. Li, D. Reinhoudt and M. Crego-Calama, *Chem. Soc. Rev.*, 2007, **36**, 1350.
25 P. Roach, N. J. Shirtcliffe and M. I. Newton, *Soft Matter*, 2008, **4**, 224.
26 M. Ma and R. M. Hill, *Curr. Opin. Colloid Interface Sci.*, 2006, **11**, 193.
27 F. Xia and L. Jiang, *Adv. Mater.*, 2008, **20**, 2842.
28 J.-L. Liu, X.-Q. Feng, G. Wang and S.-W. Yu, *J. Phys.: Condens. Matter*, 2007, **19**, 356002.
29 S. Herminghaus, *Europhys. Lett.*, 2000, **52**, 165.
30 (*a*) H. Yan, K. Kurogi, H. Mayama and K. Tsujii, *Angew. Chem., Int. Ed.*, 2005, **44**, 3453; (*b*) K. Kurogi, H. Yan, H. Mayama and K. Tsujii, *J. Colloid Interface Sci.*, 2007, **312**, 156.
31 T. Darmanin and F. Guittard, *Langmuir*, 2009, **25**, 5463.
32 T. Darmanin, N. Nicolas and F. Guittard, *Langmuir*, 2008, **24**, 9739.
33 K. Chiba, K. Kurogi, K. Monde, M. Hashimoto, M. Yoshida, H. Mayama and K. Tsujii, *Colloids Surf., A*, 2010, **354**, 234.
34 (*a*) M. Nicolas, F. Guittard and S. Geribaldi, *Angew. Chem., Int. Ed.*, 2006, **45**, 2251; (*b*) M. Nicolas, F. Guittard and S. Geribaldi, *Langmuir*, 2006, **22**, 3081.
35 T. Darmanin, M. Nicolas and F. Guittard, *Phys. Chem. Chem. Phys.*, 2008, **10**, 4322.
36 (*a*) C. Neinhuis and W. Barthlott, *Ann. Bot.*, 1997, **79**, 667; (*b*) W. Barthlott and C. Neinhuis, *Planta*, 1997, **202**, 1.
37 Z. Guo and W. Liu, *Plant Sci.*, 2007, **172**, 1103.
38 X. Gao, X. Yan, X. Yao, L. Xu, K. Zhang, J. Zhang, B. Yang and L. Jiang, *Adv. Mater.*, 2007, **19**, 2213.
39 L. Feng, Y. Zhang, J. Xi, Y. Zhu, N. Wang, F. Xia and L. Jiang, *Langmuir*, 2008, **24**, 4114.
40 Y. Miyauchi, B. Ding and S. Shiratori, *Nanotechnology*, 2006, **17**, 5151.
41 Z.-Z. Gu, H.-M. Wei, R.-Q. Zhang, G.-Z. Han, C. Pan, H. Zhang, X.-J. Tian and Z.-M. Chen, *Appl. Phys. Lett.*, 2005, **86**, 201915.
42 E. Puukilainen, T. Rasilainen, M. Suvanto and T. A. Pakkanen, *Langmuir*, 2007, **23**, 7263.
43 H. Lim, D.-H. Jung, J.-H. Noh, G.-R. Choi and W.-D. Kim, *Chin. Sci. Bull.*, 2009, **54**, 3613.
44 S. Chen, C. Hu, L. Chen and N. Xu, *Chem. Commun.*, 2007, 1919.
45 P. Tsai, S. Pacheco, C. Pirat, L. Lefferts and D. Lohse, *Langmuir*, 2009, **25**, 12293.
46 M. Madou, *Fundamentals of Microfabrication*, CRC Press, 2nd edn, 2002.
47 T. Darmanin and F. Guittard, *J. Colloid Interface Sci.*, 2009, **335**, 146.
48 E. Hosono, S. Fujihara, I. Honma and H. Zhou, *J. Am. Chem. Soc.*, 2005, **127**, 13458.
49 (*a*) A. B. D. Cassie and S. Baxter, *Trans. Faraday Soc.*, 1944, **40**, 546; (*b*) S. Baxter and A. B. D. Cassie, *J. Text. Inst., Trans.*, 1945, **36**, T67.
50 K. Kurogi, H. Yan and K. Tsujii, *Colloids Surf., A*, 2008, **317**, 592.